FACTA UNIVERSITATIS
Series: **Mechanical Engineering**
https://doi.org/10.22190/FUME220903003A

Original scientific paper

EXPERIMENTAL AND NUMERICAL INVESTIGATION ON THE PERFORMANCES OF A SMALL WEAPON BARREL DURING ITS LIFECYCLE

Walid Boukera Abaci[1], Nebojsa Hristov[1], Igor Radisavljevic[2], Lazar Stojnic[1], Aleksa Anicic[3]

[1]University of Defense in Belgrade, Military Academy, Belgrade, Serbia
[2]Military Technical Institute, Belgrade, Serbia
[3]Proof House for Experimental Testing, Kragujevac, Serbia

Abstract. *The paper presents experimental and numerical investigations on the performances of a small caliber rifle barrel during its lifecycle. Two 7.62 mm rifle barrels were used, the first was considered as a standard barrel, the second barrel was subjected to an accelerated life cycle test. Measurements of the muzzle velocity, the rate of fire and the firearm accuracy and precision were carried out. The paper presents the correlation between the measured parameters and the total number of shots fired. After the durability tests, longitudinal cross sections were made by cutting the tested and the standard barrels. 3D scanning was employed to perform a comparison between the tested and the standard bore surfaces. ANSYS Explicit dynamic analyses were performed based on the obtained surface scans. The numerical analyses results of the tested and the standard barrels showed good agreement with the experimental and the numerical internal ballistic model results.*

Key words: *Accelerated lifecycle tests, Muzzle velocity, Rate of firing, Accuracy, Precision, Bore damage, 3D scanning, Explicit dynamic analysis*

1. INTRODUCTION

The performance of weapon barrels decreases significantly during their usage. During the firing, the barrel is subjected to high thermo-mechanical stresses caused by the highly pressurized combustion gases and the interaction with the accelerated projectile. For the brief time that the firing process takes the barrel will be affected by the chemically reactive gases at elevated pressures and temperatures. Inevitable damage will occur to the internal surfaces that progress with repetitive usage of the barrel. Those damages are known as the

Received: September 03, 2022 / Accepted: January 15, 2023
Corresponding author: Nebojsa Hristov
University of Defence Belgrade, Military Academy Belgrade, Veljka Lukića Kurjaka 33, 11042 Belgrade
E-mail: (nebojsahristov@gmail.com)

wear and erosion of the barrels. Unwanted phenomena that lead to the degradation of the barrel performances. The exterior ballistic process highly depends on the initial directional and rotational muzzle velocities. Internal surface damage will affect the projectile surface topography and the initial velocities which will affect the bullet's aerodynamic parameters and induce a significant loss in the accuracy and precision of the rifle.

Much research has been established to study and predict the wear and erosion of the barrels experimentally and numerically [1-7]. Jaramaz et al. [8] have developed a laboratory apparatus and a method for determining the erosion coefficient of gunpowder both experimentally and theoretically. Abhilash et al. [9] and Johnston [10] summarized in their reviews the various studies on erosion taking place in the weapon barrel and gave a list of various methods developed over the years to calculate and mitigate the barrel wear. New research has been conducted to study the bore damage of the barrel with the use of the new numerical advanced analysis tools to accurately predict its effect.

Shen et al. [11] studied the influences of bore damage on the bullet-barrel interaction process and the end of a 12.7 mm machine gun barrel's service life. Based on the damage data obtained through barrel life tests they developed a novel finite element mesh generation method for the damaged barrel and a new transient coupled thermo-mechanical finite element (FE) model. Based on the barrel's accelerated life test, and using numerical simulation technology and the ballistic performance change at each shooting stage, Li et al. [12] reproduced the whole process of projectile shooting and established a relation between the angle of attack of the projectile and the wear of the barrel. They showed that the projectile muzzle spin rate decreases 57.5% than that of a barrel without wear. Xiaolong et al. [13] also analyzed wear mechanism at different positions in the bore and established a three-dimensional barrel-wear finite element model using a parametric modeling method and concluded that the fundamental reason for interior ballistic performance degradation was wear on the initial position of the rifling. Ding et al. [14] provided a new finite element meshing strategy for the worn barrel and a new parametric geometric modeling method for gun barrel using Python code and ABAQUS software. By considering the gases propelling force and the changing friction stress effect, the user subroutine VUAMP and VFRICTION were implemented to develop a transient coupled thermo-mechanical FE model to compute the plastic deformation of the rotating band and the performance of interior ballistics.

In order to investigate the small caliber rifle performances during the course of its lifecycle, durability tests were conducted to accelerate the barrel lifespan, measures of the initial velocity, the rate of firing and the firing accuracy and precision were taken regularly. The internal surfaces of the used and standard barrels were obtained using 3D scanning. The obtained results were used to perform explicit dynamic analyses using ANSYS software.

2. EXPERIMENTS

Two 7.62 mm automatic rifle barrels were used. The first one is a new barrel and is considered as a standard barrel. The second one is a used barrel. It was used for 8000 rounds before performing a durability test. The durability test consisted of firing a large number of shots in different regimes using a standard nitrocellulose propellant. The experiments were performed with the standard atmospheric conditions.

After every 1000 shots, a series of performance measurements were made:

- The initial velocity of the V_0 on a group of 10 shots (3 x 10 Shots)
- The rate of firing on a group of 60 shots (2 x 30 shots)
- Accuracy and precision tests on 3 targets in a group of 10 shots per target at a distance of 100 m.

During the durability test, 13,860 rounds were fired (a total of 21,900 rounds were fired from the used rifle) of ammunition 7.62 × 39 mm.

The velocity V_0 was measured using a ballistic chronograph placed 2.5 m from the muzzle. The rate of fire was determined using a measuring system based on optical and sound sensors to register the cadence. The device is an integral part of the laboratory equipment for testing ballistic characteristics in the Zastava Arms test center. The system is equipped with sound and light sensors to be able to detect the sound produced by the shot, as well as the flash from the muzzle of the weapon when fired. The time between two firing was measured with an accuracy of 1 μs. The measurement results were collected using a specific acquisition system.

The accuracy and precision of the barrels of the rifle are tested under favorable atmospheric conditions in a covered area of the shooting range protected from the wind and outside influences. Before the start of the test, parts that could affect shooting accuracy were replaced and the weapon was cleaned and then inspected. Precision and accuracy were tested by shooting 10 bullets of the same series and original packaging for each of the three targets. Targets were placed at a distance of 100 m with sight. The shooting was performed by an excellent sitting down shooter using a tactical riflescope. The aiming point was the center of the black disk of the target that should be on the weapon horizon. After shooting, the target (Fig. 1) was inspected and the coordinates of the scatter were collected.

Fig. 1 One of the three targets after shooting 10 shots at 17000 rounds

3. RESULTS OF THE EXPERIMENTS

The durability test results are summarized in Table 1.

Table 1 Durability test results

N x 10^3	0	8	9	10	11	12	13	14
V_0 [m/s]	720.21	690.83	692.02	691.18	687.61	692.58	688.40	681.84
Rate of firing [shot/min]	620	622	627	627	635.5	629	631	635.5
N x 10^3	15	16	17	18	19	20	21	
V_0 [m/s]	685.59	675.38	677.49	673.64	667.01	669.89	664.81	
Rate of firing [shot/min]	638	633.5	635	641	640.5	641	642	

Figures 2 and 3 represent the initial muzzle velocity and the rate of firing as a function of the fired round number.

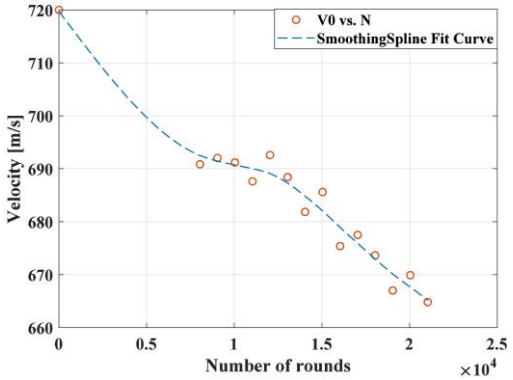

Fig. 2 Muzzle velocity vs. Number of rounds

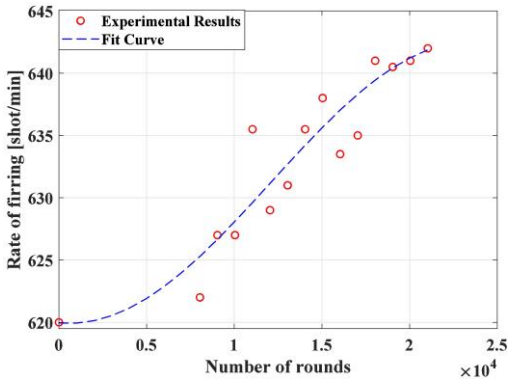

Fig. 3 Rate of fire vs. Number of rounds

The muzzle velocity experienced a decrease of 7.69% while the rate of fire experienced an increase of 3.55% between the results of the standard barrel and the results of the tested barrel after 21,800 rounds were fired.

The XY coordinates of the shots on the targets were collected and treated to obtain the coordinate of the center of shots, and the XY standard deviations of the shots as a function of the number of rounds (Figs. 4 and 5).

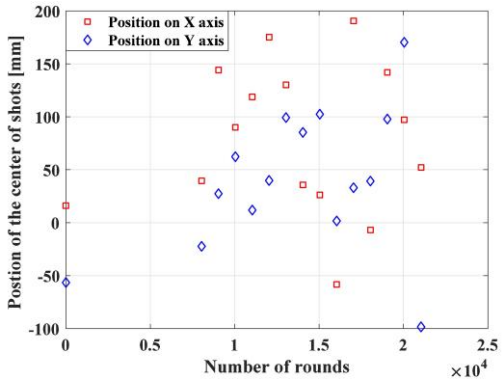

Fig. 4 Position of the center of shots vs. Number of rounds

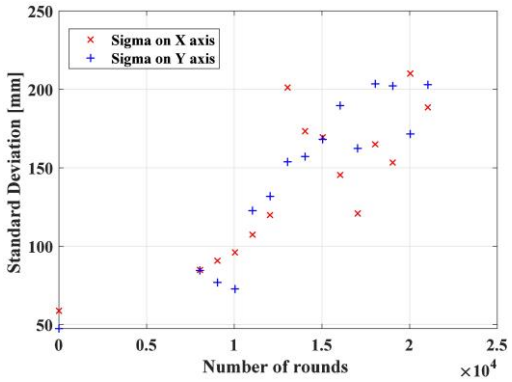

Fig. 5 Standard deviations vs. Number of rounds

The Circular Error Probable (CEP) is the radius of a circle that has a 50% probability of containing the target. The CEP of each of the measures was calculated approximately using Eq. (1), [15], the obtained results were presented in Fig. 6.

$$CEP = \begin{cases} \sigma_L (0.67 + 0.8 \times w^2) & \text{if } 0 < w < 0.5 \\ 0.59 \times \sigma_L (1 + w) & \text{if } 0.5 \le w \le 1 \end{cases} \quad \text{where} \quad \begin{cases} \sigma_L = \max(\sigma_x, \sigma_y) \\ \sigma_S = \max(\sigma_x, \sigma_y) \\ w = \sigma_S / \sigma_L \end{cases} \tag{1}$$

The accuracy of a rifle refers to how close the measurements are to the aiming point. The precision of the rifle refers to how close the measurements are to each other. The coordinate of the center of shots presented in Fig. 4, showed that the accuracy of the tested barrel was independent of the number of the total round fired. However, the precision was

affected as it is shown in Figs. 5 and 6. The standard deviation of the results and the CEP increased with the total round fired.

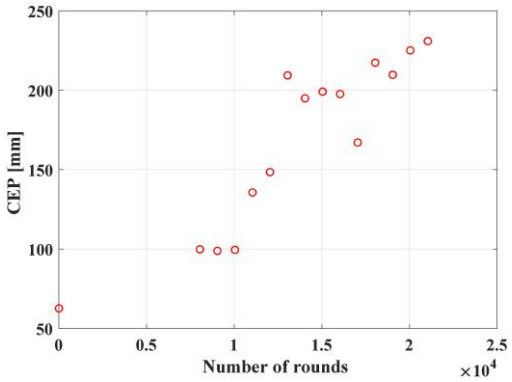

Fig. 6 CEP vs. Number of rounds

After the tests, longitudinal sections were made from the tested and the standard barrels using the wire-cut electrical discharge machining (EDM) process. The EDM process is a technique using sparks produced by electrical discharge to manufacture work-pieces in accurate dimensions and shape [16,17]. Figures 7 and 8 show the longitudinal sections of the standard barrel and the used barrel, respectively. Accurate views of the origin of rifling were obtained using an optical microscope as it can be seen in the Figs. 7 and 8.

Fig. 7 Longitudinal section of the standard barrel

Fig. 8 Longitudinal section of the tested barrel

4. LASER SCANNING OF THE INTERIOR SURFACES

For the purposes of measuring the interior surfaces and creating a 3D model, a 3D scanner Hexagon RS5 was used, with a stabilized Absolute arm platform 8525-7, shown

in Fig. 9. With a precision of 0.048 mm, this system enables the reliable determination of 3D point clouds of the inner surface for the longitudinal cross-sections of the tested and the standard barrels. The technical characteristics of the laser scanner and the stabilization platform can be found in the Hexagon brochure [18]. The RS5 laser scanner scans results of the used and the standard barrels were introduced to the POLYWORKS software where preliminary preparations were made like setting the geometries approximately in the Cartesian reference and deleting the majority of the unwanted scanned surfaces and points (Fig. 10).

The initial results were imported to Matlab developed code as STL files, in order to extract the Cartesian coordinates of the 3D scatter plot points. Points that do not belong to the barrel bore surface were removed. The XYZ coordinates of the center of two distant sections were determined using the average value of all the XYZ specific section points. The rotation and translation matrix were calculated using the resulting vector between the two sections centers. Using those rotation and translation matrixes the geometries were installed in the Cartesian coordinate system. The average distance of the lands and grooves from the barrels axes were calculated following a cylindrical helix curve. The obtained results are presented in Fig. 11.

Fig. 9 3D scanner Hexagon RS5 with a stabilized Absolute arm platform 8525-7

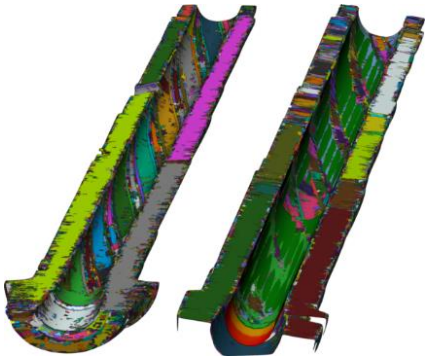

Fig. 10 3D scans of the standard (left) and tested (right) barrels

The origin of rifling was the most damaged area of the bore where the total land material was removed. This will increase the free travel distance of the projectile and delay the

proper engraving of the bullet jacket. Increasing the free travel distance will decrease the total time of the firing process, which can explain the rise in the rate of fire. The thickness of the lands decreases unevenly with a maximum loss in the average land radius value of 0.17 mm at the axial position 76 mm from the bottom of the barrel.

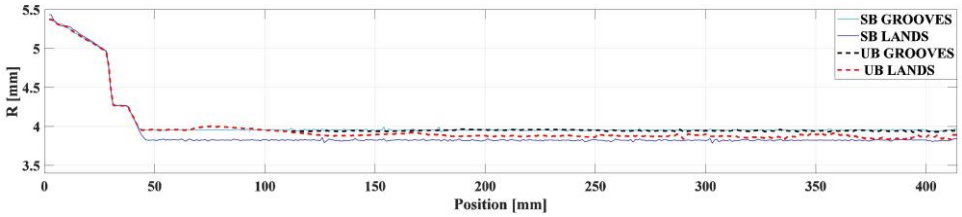

Fig. 11 Average radius of the internal surfaces (Lands and Grooves) of the used (UB) and the standard barrels (SB) as a function of the axial position

5. EXPLICIT DYNAMICS ANALYSES

Based on the 3D laser scanning data two CAD models (Fig. 12) for the standard and tasted barrels were created and used in an explicit dynamic analyses to simulate the interior ballistics process of a coupled projectile-barrel system.

The explicit dynamic analysis is used to provide a firing process model considering its short-duration and high-pressure loadings. Such a complex phenomenon requires advanced analyses tools to accurately predict its effect on the rifle and the bullet design. Creating a high-quality mesh is one of the critical factors that must be considered to ensure simulation accuracy. A high-quality mesh means that there is an optimal balance between the computational cost and the level of fineness achieved. The meshing was made in a helicoidally way for both the barrels and the bullet to match the shape of deformations.

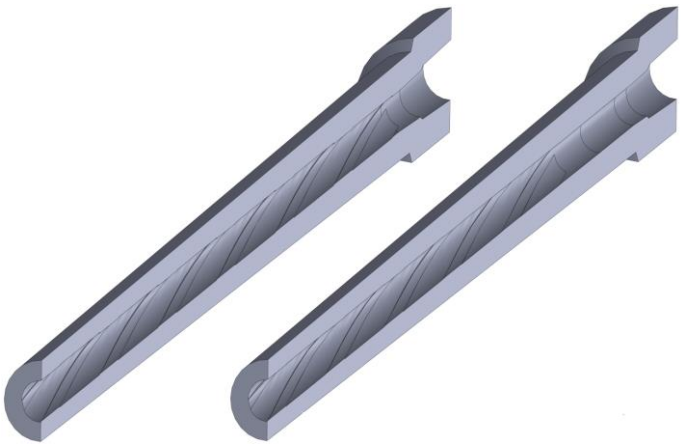

Fig. 12 CAD Models for the standard (left) and the tested (right) barrels

The three-dimensional refinement was made manually by retaining the element types and attempting to convert the elements in the regions where the interactions accrue between the barrel and the bullet into smaller elements of the same type as the original elements. This refinement effectively decreases the cell size of only the target area but does not increase the computational cost dramatically.

In order to refine the mesh in the radial, axial and azimuthal directions special transitional mesh elements (Fig. 13, left) were needed to increase the number of cells in the desired direction. More developed mesh elements (Fig. 13, right) were needed to increase the number of cells in two directions simultaneously. The whole model was used for the analyses.

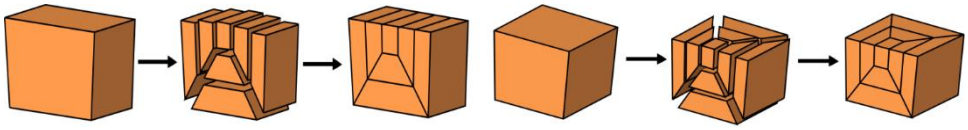

Fig. 13 Transitional mesh elements in one (left) and two (right) directions

Fig. 14 represents the HEX8 elements (8 Nodes hexahedron) mesh of only a quarter of the projectile and the barrel to show the mesh refinement in all three (XYZ) directions.

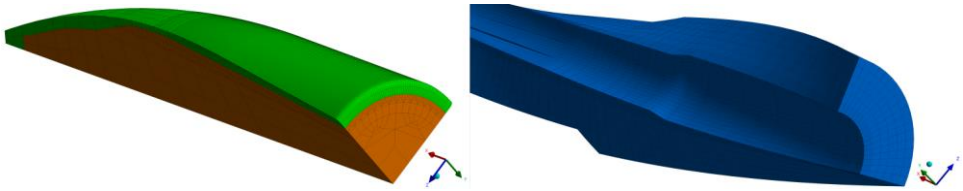

Fig. 14 Helicoidal mesh of a quarter of the (left) projectile and the (right) barrel

The number of nodes, elements and the type of elements are presented in the Table 2.

Table 2 Type and number of finite elements

Geometries	Barrels	Bullet
Number of nodes	517,932	159,435
Number of elements	446,812	143,504
Type of elements	HEX8	HEX8

The projectile core and the barrels are made of the same material (steel), which is assumed to have a linear elastic behavior. The steel mechanical and thermal properties are presented in Table 3. The projectile jacket material (brass) has a homogeneous, isotropic, elastic-plastic behavior with Johnson-Cook plastic deformation and failure models. The brass mechanical and thermal properties are summarized in Table 4. The contact between the barrel and the projectile is a frictional contact with penalties.

Table 3 Steel mechanical and thermal properties [13-14]

Parameters	E [GPa]	Poisson ratio	Density [kg/m^3]	Yield Stress [MPa]	Specific heat c_p [J/kg K]	Thermal conductivity [W/m K]
Value	206	0.31	7850	933	483	30

Table 4 Brass jacket material mechanical and thermal parameters [11]

Elastic and thermal parameters	E [GPa]	Poisson ratio	Density [kg/m^3]	Specific heat [J/kg K]		Thermal conductivity [W/m K]	
Value	115	0.31	8800	375		110	
Plastic Parameters	A [MPa]	B [MPa]	C	n	m	Tm [K]	$\dot{\varepsilon}_0$ [s^{-1}]
Value	206	505	0.01	0.42	1.68	1189	5x10^{-4}
Damage and fracture parameters	D1	D2	D3	D4		D5	
Value	0.54	4.89	-3.03	0.014		1.12	

The stresses in the barrel caused by the firing are the results of different loads. The main loads are the mechanical and thermal loads generated by the combustion of the propellant. For reasons of simplification in this study, all the loads are neglected except the stresses caused by the generated pressure of the propellant combustion and the interaction between the barrel and the bullet. Fixed support boundary condition was applied on the rear surface of the barrel. Moreover, the whole model was used, i.e. no symmetry conditions were applied.

The loads introduced to the analyses are time-space dependent loads (Fig. 15). They are applied as tabular data in a way that for each time step we introduced a pressure load applied on the interior walls of the barrel and the back of the projectile. The loads were calculated using the two-phase flow internal ballistic model presented in [19]. The two-phase flow model considers both the solid (gunpowder grains) and the combustion gaseous component during the firing process and at a given time compute different pressure values along the barrel.

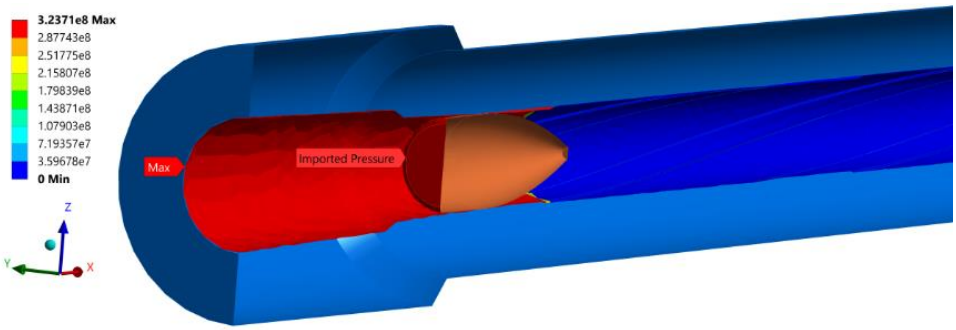

Fig. 15 Time-space dependent loads on the barrel and the projectile

6. Explicit Dynamic Analyses Results Discussion

For a reasonable comparison between the analytical and the numerical analyses, both must have the same input parameters. For that reason, the bullet was suppressed in a preliminary simulation to neglect the effect of the bullet acceleration on the barrel. The total equivalent stresses obtained by the dynamic explicit analyses are compared with the analytical stress. The analytical equivalent stress is calculated by the von Mises formula,

$$\sigma_e = \sqrt{\frac{1}{2}((\sigma_r - \sigma_t)^2 + (\sigma_r - \sigma_z)^2 + (\sigma_t - \sigma_z)^2)} \tag{2}$$

where σ_r is radial stress, σ_z is axial stress and σ_t is tangential stress [20].

Figure 16 represents the analytical and numerical equivalent total stresses as a function of the barrel radius (R) obtained in simulations with and without projectile for section 60 mm at 0.34 ms (Fig. 16, left) and section 120 mm at 0.38 ms (Fig. 16, right) from the bottom of the barrel. The equivalent stresses obtained by the simulations have the same trend as the analytical equivalent stresses for values of radii greater than 5 mm. The graphs of the simulations equivalent stresses show fluctuations for radii smaller than 5 mm, which is the region of the grooves and lands. Those fluctuations could be explained by the creation of stress concentrations created in that region [21]. The equivalent stresses obtained by the simulation without projectile showed a good match with the analytical stresses, whereas the equivalent stresses obtained by the simulation with projectile were higher than the analytical stresses due to the presence of the projectile. The rotation and translation of the projectile generate other types of stresses on the barrel, such as the axial stress and torsional stress.

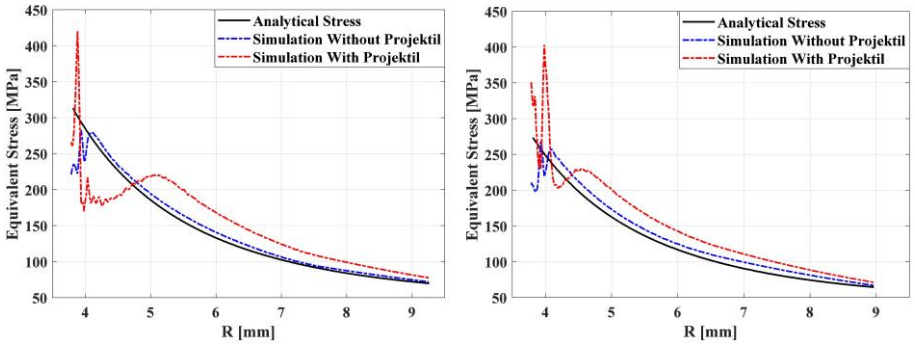

Fig. 16 Analytical and numerical equivalent total stresses for section 60 mm at 0.34 ms (left) and 120 mm at 0.38 ms (right) from the bottom of the barrel

The second and third comparisons were made between the position and the velocity of the projectile results calculated by the numerical model two-phase flow [19] and the results obtained by the explicit analysis of the standard barrel, as it is shown in Fig. 17. The projectile position and velocity results obtained by the simulation showed good match with the results obtained by the internal ballistic model.

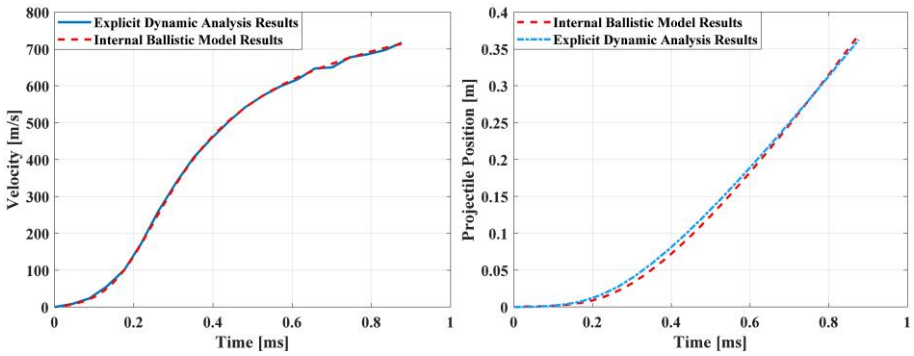

Fig. 17 Position (left) and velocity (right) of the projectile obtained by the numerical simulations and the internal ballistic model

Fig. 18 shows the position of the projectile at the end time where the projectile reaches the muzzle.

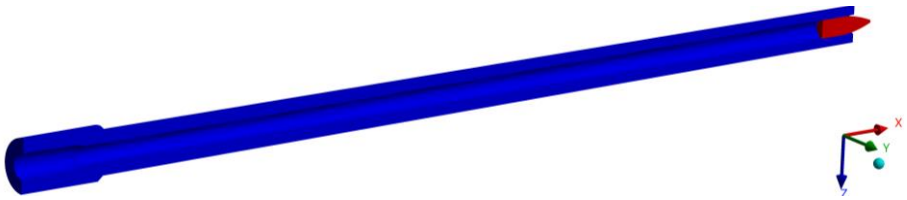

Fig. 18 Position of the bullet at the end of the simulation

Figures 19 and 20 show a comparison between the equivalent total plastic strain obtained by the simulations and the deformations of the projectiles fired by the standard and the tasted barrels after the durability test.

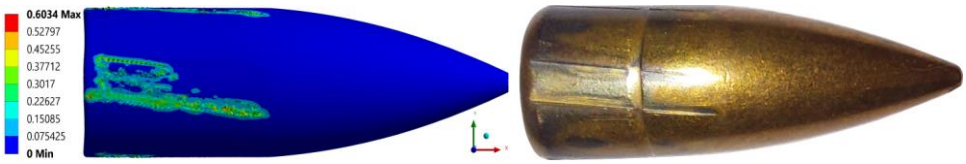

Fig. 19 Equivalent total plastic strain of the bullet fired by the standard barrel at the end of the simulation (left), experimental plastic deformations of the projectile (right)

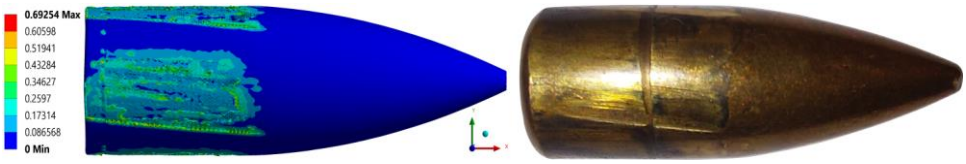

Fig. 20 Equivalent total plastic strain of the bullet fired by the used barrel at the end of the simulation (left), experimental plastic deformations of the projectile (right)

Figures 19 and 20 show apparent similarity in the shape of the plastic deformation obtained by the experiments and the explicit dynamic analyses for both tested and standard barrels.

At the beginning of the barrel lifespan, the engraving of the projectile outer surface is done at small accelerations. The uniform lands thickness is sufficient to allow the projectile to gain rotational velocity without further bullet-jacket deformation. The initial depth of the deformation will stabilize the smooth movement of the projectile on lands. However, with the continued use of the weapon, the interior surface will be deteriorated, and the thickness of the lands will decrease unevenly, the engraving of the projectile outer surface will be done far from the origin of refiling at significant accelerations. The bullet will no longer have a smooth movement on lands behavior and more azimuthal bullet-jacket deformation will occur, which will generate more vibration, more friction and material deformation energy loss, less rotational and directional velocities and a displacement from the initial spin axis.

Figure 21, left, shows the velocities of the projectiles as a function of time determined by the simulations. The projectiles velocities reached are 717.29 m/s and 669.95 m/s for the standard and tested barrel, respectively. Fig. 21, right, shows the angular velocities of the projectiles as a function of time determined by the same simulations. The projectiles angular velocities reached are 171,824 RPM and 135,786 RPM for the standard and tested barrel, respectively.

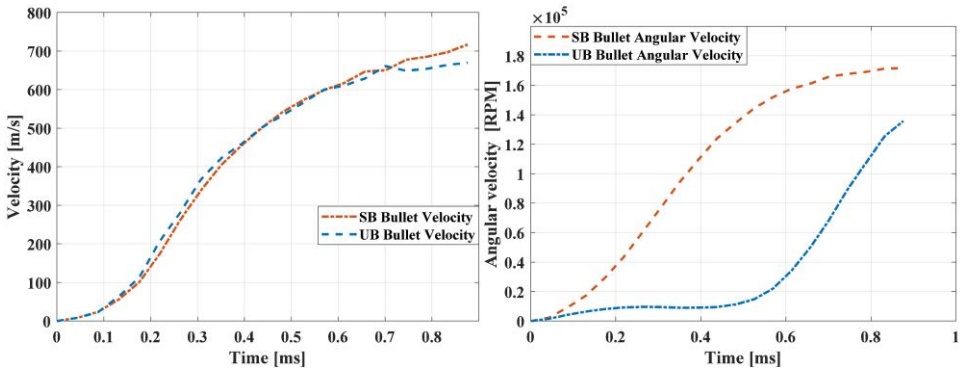

Fig. 21 (left) Projectile velocities and (right) angular velocities of the standard and tested barrels as a function of time

From the simulations results, the projectiles initial axial directional velocities drops by 6.59% and 20.97% in the projectile initial angular velocities between the standard and tasted barrels. The initial angular velocity of the projectile is crucial in the projectile flight stability and affects the rifle precision. A reduction of 20% would affect the projectile flight stability and result in a sharp decline in the firing range and precision.

Table 5 shows the initial velocities comparison between the experimental and the simulation results for both the standard and used barrels. The percentage of the difference between the experimental and the simulation velocities were less than 1% for both the standard and used barrels. The satisfactory agreements between the presented results increase the credibility of this work.

Table 5 Initial velocities comparison

	Standard barrel [m/s]	Used barrel [m/s]
Experimental results	720.21	664.82
Simulation results	717.29	669.95
Percentage of the difference Experimental vs. Simulation	0.41%	0.77%

7. CONCLUSION

The paper presented experimental and numerical investigations on the performances of a small caliber rifle barrel during its lifecycle. Durability test experimentations were conducted on a 7.62 mm automatic rifle. Appropriate measurements were made to track the rifle performances during the stages of its lifecycle.

After the durability testes, the used and the standard barrels were cut longitudinally using the wire-cut EDM process to enable the detection of the rifle's internal surfaces damage using 3D scanning. Based on the 3D scans, ANSYS explicit dynamic analyses were conducted to investigate the behavior of the tested and the standard barrels. Special transitional mesh elements were used to be able to refine the regions where the interactions accrue between the barrel and the projectile.

The following conclusions can be extracted from the experimental and simulation results:

- The tests showed correlations between the performances of the rifle and the total number of shots fired. The muzzle velocity experienced a drop of 7.66% at the end of the tests while the rate of firing experienced an increase of 3.55%. The accuracy of the firing was independent of the total round fired number. According to the standard deviation of the shots and the CEP tests the precision of the rifle decreases with the repetitive use of the weapon.
- The optical microscope images showed the degradation of the bore internal surface in the region of the origin of rifling. Moreover, according to the calculation of the average distance of the lands and grooves from the barrels axes the origin of rifling experienced the severest damage with total removal of the land material.
- The numerical analyses showed satisfactory agreements with the experimental and the internal ballistic model results. The equivalent stresses obtained by the simulation without projectile showed good agreement with the analytical stresses. The projectile position and velocity results achieved by the simulation were similar to the internal ballistic model results. Furthermore, visible similarities in the projectile surface plastic deformation were captured between the experiments and the numerical analyses. On the top of that, the differences between the experimental and the simulation velocities were less than 1% for both the standard and used barrels.
- According to the simulation results, the projectile experienced a drop of 6.59% and 20.97% in the initial and rotational velocities respectively between the standard and tasted barrels. Which also indicates the diminution of the rifle barrel performances.

The explicit dynamic analyses were employed to provide a model of the short duration firing process for the standard and tested barrels. Since it is too expensive to perform physical testing, success in modeling this process can help in the improvement of the rifle's

design. A reliable explicit dynamic analysis can accurately predict complex responses, such as large material deformations and failure and interactions between the barrel and the projectile. Based on the explicit dynamic analysis, the lifespan of the rifle barrel can be predicted more accurately.

Acknowledgement: *The research was supported by Test Center of Zastava Arms Kragujevac of the Republic of Serbia and Hexagon Manufacturing Intelligence – Hexagon Metrology Representative Office Serbia for experimental tests.*

REFERENCES

1. Ahmad, I., 1988, *The problem of gun barrel erosion: an overview*, Gun propulsion technology, 109, pp. 311-355.
2. Lawton, B., 2001, *Thermo-chemical erosion in gun barrels*, Wear, 251(1-12), pp. 827-838.
3. Lawton, B., 2003, *The influence of additives on the temperature, heat transfer, wear, fatigue life, and self ignition characteristics of a 155 mm gun*, Journal of Pressure Vessel Technology, 125(3), pp. 315-320.
4. Sopok, S., Rickard, C., Dunn, S., 2005, *Thermal–chemical–mechanical gun bore erosion of an advanced artillery system part one: theories and mechanisms*, Wear, 258(1-4), pp. 659-670.
5. Sopok, S., O'Hara, P., Pflegl, G., Dunn, S., Coats, D., 1997, *Thermochemical erosion modeling of the 25 mm M242/M791 gun system*, 33th Joint Propulsion Conference and Exhibit, 2850.
6. Sopok, S., O'Hara, P., Pflegl, G., Dunn, S., Coats, D., Nickerson, G., 1999, *Unified computer model for predicting thermochemical erosion in gun barrels*, Journal of propulsion and power, 15(4), pp. 601-612.
7. Sopok, S., O'Hara, P., Pflegl, G., Dunn, S., Coats, D., 1996, *First computer code for predicting thermochemical erosion in gun barrels*, Report ARCCB-TR-96015, Benet Weapons Lab, Watervliet, NY, USA.
8. Jaramaz, S., Micković, D., Elek, P., 2010, *Determination of gun propellants erosivity: Experimental and theoretical studies*, Experimental thermal and fluid science, 34(6), pp. 760-765.
9. Putti, A.A., Chopade, M.R., Chaudhari, P.E., 2016, *A review on gun barrel erosion*, International journal of current engineering and technology, 4, pp. 231-235.
10. Johnston, I.A., 2005, *Understanding and predicting gun barrel erosion*, Report DSTO-TR-1757, Weapons Systems Division, Australia.
11. Shen, C., Zhou, K.D., Lu, Y., Li, J.S., 2019, *Modeling and simulation of bullet-barrel interaction process for the damaged gun barrel*, Defence Technology, 15(6), pp. 972-986.
12. Li, X., Mu, L., Zang, Y., Qin, Q., 2020, *Study on performance degradation and failure analysis of machine gun barrel*, Defence Technology, 16(2), pp. 362-373.
13. Li, X., Wang, Y., Zang, Y., Guan, B., Qin, Q., 2019, *Analysis of interior ballistic performance degradation of a worn gun barrel based on finite element method*, Journal of Physics: Conference Series, 1314(1), 012090.
14. Ding, C., Liu, N., Zhang, X., 2017, *A mesh generation method for worn gun barrel and its application in projectile-barrel interaction analysis*, Finite Elements in Analysis and Design, 124, pp. 22-32.
15. Nelson, W., 1988, *Use of circular error probability in target detection*, Report ESD-TR88-109, Massachusetts, USA.
16. Akıncıoğlu, S., 2022, *Taguchi optimization of multiple performance characteristics in the electrical discharge machining of the TiGr2*, Facta Universitatis-Series Mechanical Engineering, 20(2), pp. 237-253.
17. Sidhu, A.S., 2021, *Surface texturing of non-toxic, biocompatible titanium alloys via electro-discharge*, Reports in Mechanical Engineering, 2(1), pp. 51-56.
18. www.hexagonmi.com/nl-NL/products/portable-measuring-arms/romer-absolute-arm-compact (last access: 08.08.2022)
19. Boukera Abaci, W., Hristov, N. P., Ziane, A. N., Jerković, D. D., Savić, S. R., 2021, *Analysis of thermal and gas-dynamic characteristics of different types of propellant in small weapons*, Thermal Science, 25(6 Part A), pp. 4295-4306.
20. Evci, C. Isik, H., 2018, *Analysis of the effect of propellant temperature on interior ballistics problem*, Journal of Thermal Engineering, 4(4), pp. 2127-2136.
21. Boukera Abaci, W., Kari, A.V., Jerković, D.D., Hristov, N.P., 2020, *The influence of the internal ballistic pressure on the rifled barrel stress response*, Scientific Technical Review, 70(2), pp. 41-46.